New Approach to Parton Shower MC's for Precision QCD Theory: HERWIRI1.0(31)

S. Joseph[a], S. Majhi[b], B.F.L. Ward[a], S. A. Yost[c]

[a]*Department of Physics, Baylor University, Waco, TX 76798, USA*
[b]*Theory Division, Saha Institute of Nuclear Physics, Kolkata 700 064, India*
[c]*Department of Physics, The Citadel, Charleston, SC 29409, USA*

Abstract

By implementing the new IR-improved Dokshitzer-Gribov-Lipatov-Altarelli-Parisi-Callan-Symanzik (DGLAP-CS) kernels recently developed by one of us in the HERWIG6.5 environment we generate a new MC, HERWIRI1.0(31), for hadron-hadron scattering at high energies. We use MC data to illustrate the comparison between the parton shower generated by the standard DGLAP-CS kernels and that generated by the new IR-improved DGLAP-CS kernels. The interface to MC@NLO, MC@NLO/HERWIRI, is illustrated. Comparisons with FNAL data and some discussion of possible implications for LHC phenomenology are also presented.

1   Introduction

In the era of the LHC, we must deal with requirements of precision QCD, which entails predictions for QCD processes at the total precision [1] tag of 1% or better, where by total precision of a theoretical prediction we mean the technical and physical precisions combined in quadrature or otherwise as appropriate. We accordingly need resummed $\mathcal{O}(\alpha_s^2 L^n), \mathcal{O}(\alpha_s \alpha L^{n'}), \mathcal{O}(\alpha^2 L^{n''})$ corrections for $n = 0, 1, 2$, $n' = 0, 1, 2$, $n'' = 1, 2$, in the presence of parton showers, on an event-by-event basis, without double counting and with exact phase space. Essential large QED and EW effects [2–4] are handled by the simultaneous resummation of large QED and QCD infrared(IR) effects, QED⊗QCD resummation [5] in the presence of parton showers, to be realized on an event-by-event basis by Monte Carlo (MC) event generator methods. Indeed, we know from Refs. [3,4] that no precision prediction for a hard LHC process at the 1% level can be complete without taking the large EW corrections into account.

In what follows, we present the first step in realizing our new MC event generator approach to precision LHC physics with amplitude-based QED⊗QCD resummation by introducing the attendant new parton shower MC for QCD that follows from our approach. We recall that in Refs. [6] our resummed QED MC methods, based on the theory in Ref. [7], are already well developed and checked in LEP1 and LEP2 precision physics applications. This means that what we do here will set the stage for the complete implementation, via MC methods, the QED⊗QCD resummed theory in which all IR singularities are canceled to all orders in α_s and α. As we will show directly, this new parton shower MC, which is developed in the HERWIG6.5 [8] environment and which we have called HERWIRI1.0(31) [9][1], already shows improvement in comparison with the FNAL soft p_T data on single Z production as we quantify below. On the theoretical side, while the explicit IR cut-offs in the HERWIG6.5 environment will not be removed here, our new shower MC only involves integrable distributions for its real emission so that in principle these cut-offs could be removed. We discuss this point further below as well.

Our discussion here proceeds as follows. We first review our approach to resummation and its relationship to those in Refs. [10,11]. Section 3 contains a presentation of the attendant new IR-improved DGLAP-CS [12,13] theory [14,15]. Section 4 features the

---

[1]We stress that we are completely replacing all the parton shower kernels in HERWIG6.5 that generate real QCD radiation and all the Sudakov form factors in HERWIG6.5 that realize the attendant virtual corrections with the new forms that follow from the results in Sections 2 and 3, together with the auxiliary functions required for these new forms, so that the parton shower physics, distributions and MC behavior are all fundamentally different from what is in HERWIG6.5. The attendant implementation has been carried out in agreement with and in close collaboration with B. Webber and M. Seymour, principal authors of the HERWIG6.5, who have also instructed us on the proper naming and references for the resulting program as we further highlight in the discussion below.

implementation of the new IR-improved kernels in the framework of HERWIG6.5 [8] to arrive at the new, IR-improved parton shower MC HERWIRI1.0(31). We illustrate the effects of the IR-improvement first with the generic 2→2 processes at LHC energies and then with the specific single Z production process at LHC energies. We compare with recent data from FNAL to make direct contact with observation. Section 5 summarizes our discussion.

For reference purposes and to put the discussion in the proper perspective with regard to what has already been achieved in the relevant literature, we note that the authors in Refs. [16,17] have argued that the current state-of-the-art theoretical precision tag on single Z production at the LHC is $(4.1 \pm 0.3)\% = (1.51 \pm 0.75)\%(QCD) \oplus 3.79(PDF) \oplus 0.38 \pm 0.26(EW)\%$ and that the analogous estimate for single W production is $\sim 5.7\%$. We continue to emphasize that these estimates show how much more work is still needed to achieve the desired 1.0% total precision tag on these two processes, for example.

2 QED⊗QCD Resummation

We follow here the discussion in Refs. [5,14,15], wherein we have derived the following expression for the hard cross sections in the SM $SU_{2L} \times U_1 \times SU_3^c$ EW-QCD theory

$$
\begin{aligned}
d\hat{\sigma}_{\exp} = {} & e^{\mathrm{SUM_{IR}(QCED)}} \sum_{n,m=0}^{\infty} \frac{1}{n!m!} \int \frac{d^3p_2}{p_2^0} \frac{d^3q_2}{q_2^0} \prod_{j_1=1}^{n} \frac{d^3k_{j_1}}{k_{j_1}} \prod_{j_2=1}^{m} \frac{d^3k'_{j_2}}{k'_{j_2}} \\
& \times \int \frac{d^4y}{(2\pi)^4} e^{iy\cdot(p_1+q_1-p_2-q_2-\sum k_{j_1}-\sum k'_{j_2})+D_{\mathrm{QCED}}} \tilde{\bar{\beta}}_{n,m}(k_1,\ldots,k_n;k'_1,\ldots,k'_m),
\end{aligned}
\tag{1}
$$

where the new YFS-style [7] residuals $\tilde{\bar{\beta}}_{n,m}(k_1,\ldots,k_n;k'_1,\ldots,k'_m)$ have n hard gluons and m hard photons and we show the final state with two hard final partons with momenta p_2, q_2 specified for a generic 2f final state for definiteness. The infrared functions $\mathrm{SUM_{IR}(QCED)}$, D_{QCED} are defined in Refs. [5,14,15]. Eq. (1) is an exact implementation of amplitude-based simultaneous resummation of QED and QCD large IR effects valid to all orders in α and in α_s. When restricted to its QED aspect, it is the basis of the well established YFS MC approach [6] to precision multiple photon radiative effects that is well tested already in LEP1 and LEP2 precision physics applications. Thus what we present in this paper, the first realization of the new parton shower MC for QCD that follows from the QCD aspect of (1), opens the way to the full MC implementation of all aspects of our QED⊗QCD resummatiom theory approach to precision LHC physics predictions.

The approach to QCD resummation contained in (1) is fully consistent with that of Refs. [10, 11] as follows. First, Ref. [18] has shown that the latter two approaches are equivalent. We show in Refs. [14, 15] that our approach is consistent with that of Refs. [10] by exhibiting the transformation prescription from the resummation formula for the theory in Refs. [10] for the generic $2 \to n$ parton process as given in Ref. [19] to our theory as given for QCD by restricting Eq. (1) to its QCD component, where a key point is to use the color-spin density matrix formulation of our residuals to capture the respective full quantum mechanical color-spin correlations in the results in Ref. [19]. For completeness, we let us recapitulate the essence of the attendant discussion here, as the arguments are not generally well-known. More precisely, to illustrate the relationship between our approach and that in Refs. [10], we use as a vehicle Ref. [19], which treats the $2 \to n$ parton process in the resummation theory of Refs [10], working in the IR and collinear regime to exact 2-loop order. The authors in Ref. [19] have arrived at the following representation for the amplitude for a general $2 \to n$ parton process [f] at hard scale Q, $f_1(p_1, r_1) + f_2(p_2, r_2) \to f_3(p_3, r_3) + f_4(p_4, r_4) + \cdots + f_{n+2}(p_{n+2}, r_{n+2})$, where the p_i, r_i label 4-momenta and color indices respectively, with all parton masses set to zero (so in our approach, we should have in mind that the masses of the quarks (see the discussion below) and the IR regulator mass of the gluon would all be taken to zero or, we could, as it is done Ref. [19], just set all masses to zero at the outset and use dimensional regularization to define both collinear and IR singular integrals)

$$
\begin{aligned}
\mathcal{M}_{\{r_i\}}^{[f]} &= \sum_L^C \mathcal{M}_L^{[f]}(c_L)_{\{r_i\}} \\
&= J^{[f]} \sum_L^C S_{LI} H_I^{[f]}(c_L)_{\{r_i\}},
\end{aligned}
\tag{2}
$$

where repeated indices are summed, and the functions $J^{[f]}$, S_{LI}, and $H_I^{[f]}$ are respectively the jet function, the soft function which describes the exchange of soft gluons between the external lines, and the hard coefficient function. The latter functions' infrared and collinear poles have been calculated to 2-loop order in Refs. [19]. How do these results relate to eq.(1)?

To make contact between eqs.(1,2), identify in the specific application $\bar{Q}'Q \to \bar{Q}'''Q'' + m(G)$ in (1) $f_1 = Q, f_2 = \bar{Q}', f_3 = Q'', f_4 = \bar{Q}''', \{f_5, \cdots, f_{n+2}\} = \{G_1, \cdots, G_m\}$,in (2), where we use the obvious notation for the gluons here. This means that $n = m+2$. Then, to use eq.(2) in eq.(1), one simply has to observe the following:

I. By its definition in eq.(2.23) of Ref. [19], the anomalous dimension of the matrix S_{LI} does not contain any of the diagonal effects described by our infrared functions $\mathrm{SUM_{IR}(QCD)}$ and D_{QCD}, where

$$
\mathrm{SUM_{IR}(QCD)} = 2\alpha_s \Re B_{QCD} + 2\alpha_s \tilde{B}_{QCD}(K_{\max}),
$$

$$2\alpha_s \tilde{B}_{QCD}(K_{\max}) = \int \frac{d^3k}{k^0} \tilde{S}_{QCD}(k)\theta(K_{\max} - k),$$

$$D_{QCD} = \int \frac{d^3k}{k} \tilde{S}_{QCD}(k) \left[e^{-iy \cdot k} - \theta(K_{\max} - k) \right], \qquad (3)$$

, where the real IR emission function $\tilde{S}_{QCD}(k)$ and the virtual IR function $\Re B_{QCD}$ are defined eqs.(77,73) in Ref. [14]. Note that (1) is independent of K_{max}.

II. By its definition in eqs.(2.5) and (2.7) of Ref. [19], the jet function $J^{[f]}$ contains the exponential of the virtual infrared function $\alpha_s \Re B_{QCD}$, so that we have to take care that we do not double count when we use (2) in (1) and in the equations in Refs. [5, 14, 15] that lead thereto.

When we observe these two latter points, we get the following realization of our approach using the results in Ref. [19]: In our result in eq.(75) in Ref. [14] for the contribution to (1) of m-hard gluons for the process under study here,

$$d\hat{\sigma}^m = \frac{e^{2\alpha_s \Re B_{QCD}}}{m!} \int \prod_{j=1}^{m} \frac{d^3k_j}{(k_j^2 + \lambda^2)^{1/2}} \delta(p_1 + q_1 - p_2 - q_2 - \sum_{i=1}^{m} k_i)$$

$$\bar{\rho}^{(m)}(p_1, q_1, p_2, q_2, k_1, \cdots, k_m) \frac{d^3 p_2 d^3 q_2}{p_2^0 q_2^0}, \qquad (4)$$

we can identify the residual $\bar{\rho}^{(m)}$ as follows:

$$\bar{\rho}^{(m)}(p_1, q_1, p_2, q_2, k_1, \cdots, k_m) = \overline{\sum}_{colors,spin} |\mathcal{M}_{\{r_i\}}^{[f]}|^2$$

$$\equiv \sum_{spins,\{r_i\},\{r_i'\}} \mathfrak{h}_{\{r_i\}\{r_i'\}}^{cs} |\bar{J}^{[f]}|^2 \sum_{L=1}^{C} \sum_{L'=1}^{C} S_{LI}^{[f]} H_I^{[f]}(c_L)_{\{r_i\}} \left(S_{L'I'}^{[f]} H_{I'}^{[f]}(c_{L'})_{\{r_i'\}} \right)^{\dagger},$$

$$(5)$$

where here we defined $\bar{J}^{[f]} = e^{-\alpha_s \Re B_{QCD}} J^{[f]}$, and we introduced the color-spin density matrix for the initial state, $\mathfrak{h}^{cs}$, so that $\mathfrak{h}_{\{r_i\}\{r_i'\}}^{cs} = \mathfrak{h}_{\{r_1, r_2\}\{r_1', r_2'\}}^{cs}$, suppressing the spin indices, i.e., $\mathfrak{h}^{cs}$ only depends on the initial state colors and has the obvious normalization implied by (4). Proceeding then according to the steps in Ref. [14] leading from (4) to (1) restricted to QCD, we get the corresponding implementation of the results in Ref. [19] in our approach, without any double counting of effects.

3 IR-Improved DGLAP-CS Theory

We show in Refs. [14, 15] that the result Eq. (1) restricted to QCD allows us to improve in the IR regime the kernels in DGLAP-CS [12, 13] theory as follows, using a standard

notation:

$$P_{qq}^{exp}(z) = C_F F_{\mathrm{YFS}}(\gamma_q)e^{\frac{1}{2}\delta_q}\left[\frac{1+z^2}{1-z}(1-z)^{\gamma_q} - f_q(\gamma_q)\delta(1-z)\right],$$

$$P_{Gq}^{exp}(z) = C_F F_{\mathrm{YFS}}(\gamma_q)e^{\frac{1}{2}\delta_q}\frac{1+(1-z)^2}{z}z^{\gamma_q},$$

$$P_{GG}^{exp}(z) = 2C_G F_{\mathrm{YFS}}(\gamma_G)e^{\frac{1}{2}\delta_G}\{\frac{1-z}{z}z^{\gamma_G} + \frac{z}{1-z}(1-z)^{\gamma_G}$$

$$+ \frac{1}{2}(z^{1+\gamma_G}(1-z) + z(1-z)^{1+\gamma_G}) - f_G(\gamma_G)\delta(1-z)\},$$

$$P_{qG}^{exp}(z) = F_{\mathrm{YFS}}(\gamma_G)e^{\frac{1}{2}\delta_G}\frac{1}{2}\{z^2(1-z)^{\gamma_G} + (1-z)^2 z^{\gamma_G}\}, \tag{6}$$

where the superscript "exp" indicates that the kernel has been resummed as predicted by Eq. (1) when it is restricted to QCD alone and where

$$\gamma_q = C_F\frac{\alpha_s}{\pi}t = \frac{4C_F}{\beta_0}, \qquad \delta_q = \frac{\gamma_q}{2} + \frac{\alpha_s C_F}{\pi}(\frac{\pi^2}{3} - \frac{1}{2}),$$

$$f_q(\gamma_q) = \frac{2}{\gamma_q} - \frac{2}{\gamma_q+1} + \frac{1}{\gamma_q+2},$$

$$\gamma_G = C_G\frac{\alpha_s}{\pi}t = \frac{4C_G}{\beta_0}, \qquad \delta_G = \frac{\gamma_G}{2} + \frac{\alpha_s C_G}{\pi}(\frac{\pi^2}{3} - \frac{1}{2}),$$

$$f_G(\gamma_G) = \frac{n_f}{6C_G F_{\mathrm{YFS}}(\gamma_G)}e^{-\frac{1}{2}\delta_G} + \frac{2}{\gamma_G(1+\gamma_G)(2+\gamma_G)} + \frac{1}{(1+\gamma_G)(2+\gamma_G)} \tag{7}$$

$$+ \frac{1}{2(3+\gamma_G)(4+\gamma_G)} + \frac{1}{(2+\gamma_G)(3+\gamma_G)(4+\gamma_G)},$$

$$F_{\mathrm{YFS}}(\gamma) = \frac{e^{-C\gamma}}{\Gamma(1+\gamma)}, \qquad C = 0.57721566..., \tag{8}$$

where $\Gamma(w)$ is Euler's gamma function and C is Euler's constant. We use a one-loop formula for $\alpha_s(Q)$, so that

$$\beta_0 = 11 - \frac{2}{3}n_f,$$

where n_f is the number of active quark flavors and $C_F = 4/3$ and $C_G = 3$ are the respective quadratic Casimir invariants for the quark and gluon color representations.

For the sake of completeness, let us illustrate how one applies the result in (1) to obtain the results in (6). We use the example of P_{qq} for definiteness. We apply the QCD exponentiation master formula embedded in eq.(1) to the gluon emission transition that corresponds to $P_{qq}(z)$, i.e., to the squared amplitude for $q \to q(z) + G(1-z)$ so that in the specialized case already discussed above one replaces everywhere the squared amplitudes for $\bar{Q}'Q \to \bar{Q}'''Q''$ processes with those for the former one plus its nG analogs with the attendant changes in the phase space and kinematics dictated by the standard methods; this implies that in eq.(53) of the first paper in Ref. [12] we have from the application of the QCD aspect of eq.(1) the replacement (see Fig. 1)
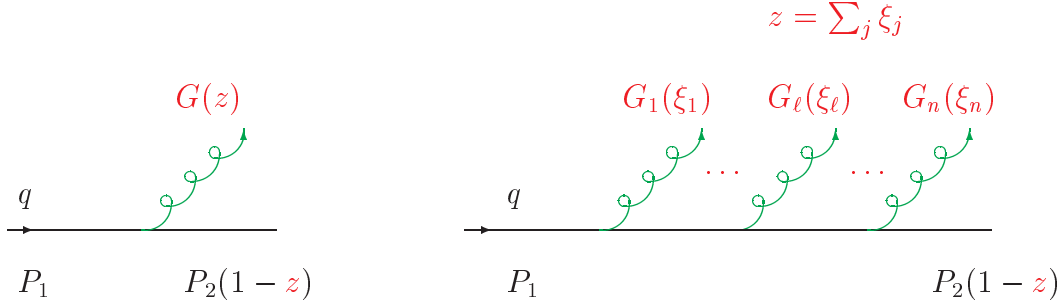
$$z = \sum_j \xi_j$$

$$G(z) \quad\quad\quad\quad G_1(\xi_1) \quad G_\ell(\xi_\ell) \quad G_n(\xi_n)$$

$$q \quad\quad\quad\quad\quad\quad\quad q$$

$$P_1 \quad\quad P_2(1-z) \quad\quad P_1 \quad\quad\quad\quad\quad\quad P_2(1-z)$$

(a)   (b)

Figure 1: In (a), we show the usual process $q \to q(1-z) + G(z)$; in (b), we show its multiple gluon improvement $q \to q(1-z) + G_1(\xi_1) + \cdots + G_n(\xi_n)$, $z = \sum_j \xi_j$.

$$P_{BA} = P_{BA}^0 \equiv \frac{1}{2}z(1-z)\overline{\sum_{spins}} \frac{|V_{A\to B+C}|^2}{p_\perp^2}$$

$$\Rightarrow \tag{9}$$

$$P_{BA} = \frac{1}{2}z(1-z)\overline{\sum_{spins}} \frac{|V_{A\to B+C}|^2}{p_\perp^2} z^{\gamma_q} F_{YFS}(\gamma_q)e^{\frac{1}{2}\delta_q}$$

where $A = q$, $B = G$, $C = q$ and $V_{A\to B+C}$ is the lowest order amplitude for $q \to G(z) + q(1-z)$, so that we get the un-normalized exponentiated result [14, 15]

$$P_{qq}(z) = C_F F_{YFS}(\gamma_q)e^{\frac{1}{2}\delta_q}\frac{1+z^2}{1-z}(1-z)^{\gamma_q}. \tag{10}$$

We see immediately that the exponentiation has removed the unintegrable IR divergence at $z = 1$. For reference, we note that we have in (10) resummed the terms[2] $\mathcal{O}(\ln^k(1-z)t^\ell\alpha_s^n)$, $n \geq \ell \geq k$, which originate in the IR regime and which exponentiate. The important point is that we have not dropped outright the terms that do not exponentiate but have organized them into the residuals $\tilde{\bar{\beta}}_m$ in the analog of eq.(1).

The application of eq.(1) to obtain eq.(10) proceeds as follows. First, the exponent in the exponential factor in front of the expression on the RHS of eq.(1) when restricted

---

[2]Following the standard LEP Yellow Book [20] convention, we do not include the order of the first nonzero term in counting the order of its higher order corrections.

to QCD is readily seen to be , using the known results for the respective real and virtual infrared functions from Refs. [14, 15],

$$SUM_{IR}(QCD) = 2\alpha_s \Re B_{QCD} + 2\alpha_s \tilde{B}_{QCD}(K_{\max})$$
$$= \frac{1}{2}\left(2C_F \frac{\alpha_s}{\pi} t \ln \frac{K_{max}}{E} + C_F \frac{\alpha_s}{2\pi} t + \frac{\alpha_s C_F}{\pi}(\frac{\pi^2}{3} - \frac{1}{2})\right) \tag{11}$$

where on the RHS of the last result we have already applied the DGLAP-CS synthesization procedure as prescribed in Refs. [14,15] to remove the collinear singularities, $\ln \Lambda_{QCD}^2/m_q^2 - 1$, in accordance with the standard QCD factorization theorems [21]. This means that, identifying the LHS of eq.(1) as the sum over final states and average over initial states of the respective process divided by the incident flux and replacing that incident flux by the respective initial state density according to the standard methods for the process $q \to q(1-z) + G(z)$, occurring in the context of a hard scattering at scale Q as it is for eq.(53) in the first paper in Ref. [12], the soft gluon effects for energy fraction $< z \equiv K_{max}/E$ give the result, from eq.(1) restricted to QCD, that, working through to the $\tilde{\bar{\beta}}$-level and using q_2 to represent the momentum conservation via the other degrees of freedom for the attendant hard process,

$$\int \frac{\alpha_s(t)}{2\pi} P_{BA} dt dz = e^{\text{SUM}_{IR}(\text{QCD})(z)} \int \{\tilde{\bar{\beta}}_0 \int \frac{d^4 y}{(2\pi)^4} e^{\{iy\cdot(p_1-p_2)+\int^{k<K_{max}} \frac{d^3k}{k} \tilde{S}_{\text{QCD}}(k)[e^{-iy\cdot k}-1]\}}$$
$$+ \int \frac{d^3 k_1}{k_1} \tilde{\bar{\beta}}_1(k_1) \int \frac{d^4 y}{(2\pi)^4} e^{\{iy\cdot(p_1-p_2-k_1)+\int^{k<K_{max}} \frac{d^3k}{k} \tilde{S}_{\text{QCD}}(k)[e^{-iy\cdot k}-1]\}}$$
$$+ \cdots \} \frac{d^3 p_2}{p_2^0} \frac{d^3 q_2}{q_2^0}$$
$$= e^{\text{SUM}_{IR}(\text{QCD})(z)} \int \{\tilde{\bar{\beta}}_0 \int_{-\infty}^{\infty} \frac{dy}{(2\pi)} e^{\{iy\cdot(E_1-E_2)+\int^{k<K_{max}} \frac{d^3k}{k} \tilde{S}_{\text{QCD}}(k)[e^{-iyk}-1]\}}$$
$$+ \int \frac{d^3 k_1}{k_1} \tilde{\bar{\beta}}_1(k_1) \int_{-\infty}^{\infty} \frac{dy}{(2\pi)} e^{\{iy\cdot(E_1-E_2-k_1^0)+\int^{k<K_{max}} \frac{d^3k}{k} \tilde{S}_{\text{QCD}}(k)[e^{-iy\cdot k}-1]\}}$$
$$+ \cdots \} \frac{d^3 p_2}{p_2^0 q_2^0} \tag{12}$$

where we set $E_i = p_i^0$, $i = 1, 2$ and the real infrared function $\tilde{S}_{\text{QCD}}(k)$ is known as well:

$$\tilde{S}_{\text{QCD}}(k) = -\frac{\alpha_s C_F}{8\pi^2}\left(\frac{p_1}{kp_1} - \frac{p_2}{kp_2}\right)^2 |_{\text{DGLAP-CS synthesized}} \tag{13}$$

and we indicate as above that the DGLAP-CS synthesization procedure as prescribed in Refs. [14, 15] is to be applied to its evaluation to remove its collinear singularities; we are using the kinematics of the first paper in Ref. [12] in their computation of $P_{BA}(z)$ in their eq.(53), so that the relevant value of $k_\perp^2$ is indeed Q^2. It means that the computation can also be seen to correspond to computing the IR function for the standard t-channel

kinematics and taking $\frac{1}{2}$ of the result to match the single line emission in P_{Gq}. The two integrals needed in (12) were already studied in Ref. [7]:

$$
\begin{aligned}
I_{YFS}(zE,0) &= \int_{-\infty}^{\infty} \frac{dy}{2\pi} e^{[iy(zE)+\int^{k<zE} \frac{d^3k}{k} \tilde{S}_{QCD}(k)(e^{-iyk}-1)]} \\
&= F_{YFS}(\gamma_q) \frac{\gamma_q}{zE} \\
I_{YFS}(zE,k_1) &= \int_{-\infty}^{\infty} \frac{dy}{2\pi} e^{[iy(zE-k_1)+\int^{k<zE} \frac{d^3k}{k} \tilde{S}_{QCD}(k)(e^{-iyk}-1)]} \\
&= (\frac{zE}{zE-k_1})^{1-\gamma_q} I_{YFS}(zE,0)
\end{aligned}
\tag{14}
$$

When we introduce the results in (14) into (12) we can identify the factor

$$
\int \left(\tilde{\bar{\beta}}_0 \frac{\gamma_q}{zE} + \int dk_1 k_1 d\Omega_1 \tilde{\bar{\beta}}_1(k_1) (\frac{zE}{zE-k_1})^{1-\gamma_q} \frac{\gamma_q}{zE} \right) \frac{d^3p_2}{E_2 q_2^0} = \int dt \frac{\alpha_s(t)}{2\pi} P_{BA}^0 dz + \mathcal{O}(\alpha_s^2).
\tag{15}
$$

where P_{BA}^0 is the unexponentiated result in the first line of (9). This leads us finally to the exponentiated result in the second line of (9) by elementary differentiation:

$$
P_{BA} = P_{BA}^0 z^{\gamma_q} F_{YFS}(\gamma_q) e^{\frac{1}{2}\delta_q}
\tag{16}
$$

Let us stress the following. In this paper, we have retained for pedagogical reasons the dominant terms in the resummation which we use for the kernels. The result in the first line of (12) is exact and can be used to include all higher order resummation effects systematically as desired. Moreover, we have taken a one-loop representation of α_s for illustration and have set it to a fixed-value on the RHS of (12), so that, thereby, we are dropping further possible sub-leading higher order effects, again for reasons of pedagogy. It is straight forward to include these effects as well – see Refs. [14,15] for more discussion on this point. Repeating the exhibited resummation calculation for the other kernels leads to the results in (6). The latter results have now been implemented by MC methods, as we exhibit in the following sections.

We stress that the improvement in Eq. (6) should be distinguished from the also important resummation in parton density evolution for the "$z \to 0$" regime, where Regge asymptotics obtain – see for example Ref. [22,23]. This latter improvement must also be taken into account for precision LHC predictions.

Let us now recall that already a number of illustrative results and implications of the new kernels have been presented in Refs. [14,15,24] which we summarize here as follows for the sake of completeness. Firstly, we note that the connection to the higher order

8

kernels in Refs. [25] has been made in Ref. [14]. This opens the way for the systematic improvement of the results presented herein. Secondly, in the NS case, we find [14] that the $n = 2$ moment is modified by $\sim 5\%$ when evolved with Eq. (6) from 2GeV to 100GeV with $n_f = 5$ and $\Lambda_{QCD} \cong 0.2\text{GeV}$, for illustration. This effect is thus relevant to the expected precision of the HERA final data analysis [26]. Thirdly, we have been able to use Eq. (1) to resolve the violation [27, 28] of Bloch-Nordsieck cancellation in ISR(initial state radiation) at $\mathcal{O}(\alpha_s^2)$ for massive quarks [29]. This opens the way to include realistic quark masses as we introduce the higher order EW corrections in the presence of higher order QCD corrections – note that the radiation probability in QED at the hard scale Q involves the logarithm $\ln(Q^2/m_q^2)$, and it will not do to set $m_q = 0$ to analyze these effects in a fully exclusive, differential event-by-event calculation of the type that we are constructing. Fourthly, the threshold resummation implied by Eq. (1) for single Z production at LHC shows a 0.3% QED effect and agrees with known exact results in QCD – see Refs. [5, 30, 31]. Fifthly, we have a new scheme [15] for precision LHC theory: in an obvious notation,

$$\sigma = \sum_{i,j} \int dx_1 dx_2 F_i(x_1) F_j(x_2) \hat{\sigma}(x_1 x_2 s) = \sum_{i,j} \int dx_1 dx_2 F'_i(x_1) F'_j(x_2) \hat{\sigma}'(x_1 x_2 s), \quad (17)$$

where the primed quantities are associated with Eq. (6) in the standard QCD factorization calculus. Sixthly, we have [5] an attendant shower/ME matching scheme, wherein, for example, in combining Eq. (1) with HERWIG [8], PYTHIA [32], MC@NLO [33] or new shower MC's [34], we may use either p_T-matching or shower-subtracted residuals $\{\hat{\tilde{\bar{\beta}}}_{n,m}(k_1, \ldots, k_n; k'_1, \ldots, k'_m)\}$ to create a paradigm without double counting that can be systematically improved order-by order in perturbation theory – see Refs. [5].

The stage is set for the full MC implementation of our QED⊗QCD resummation approach. We turn next to an important initial stage of this implementation – that of the kernels in Eq. (6).

4   MC Realization of IR-Improved DGLAP-CS Theory

In this section we describe the implementation of the new IR-improved kernels in the HERWIG6.5 environment, which results in a new MC, which we denote by HERWIRI1.0, which stands for "high energy radiation with IR improvement" [35]

Specifically, our approach can be summarized as follows. We modify the kernels in the HERWIG6.5 module HWBRAN and in the attendant related modules [36] with the following substitutions:

$$\text{DGLAP-CS } P_{AB} \Rightarrow \text{IR-I DGLAP-CS } P_{AB}^{exp} \quad (18)$$

while leaving the hard processes alone for the moment. We have in progress [37]the inclusion of YFS synthesized electroweak modules from Refs. [6]for HERWIG6.5, HERWIG++ [38] hard processes, as the CTEQ [39] and MRST(MSTW) [40] best (after 2007) parton densities do not include the precision electroweak higher order corrections that do enter in a 1% precison tag budget for processes such as single heavy gauge boson production in the LHC environment [3].

For definiteness, let us illustrate the implementation by an example [41, 42], which for pedagogical reasons we will take as a simple leading log shower component with a virtuality evolution variable, with the understanding that in HERWIG6.5 the shower development is angle ordered [41] so that the evolution variable is actually $\sim E\theta$ where θ is the opening angle of the shower as defined in Ref. [41] for a parton initial energy E. In this pedagogical example, which we take from Ref. [41], the probability that no branching occurs above virtuality cutoff Q_0^2 is $\Delta_a(Q^2, Q_0^2)$ so that

$$d\Delta_a(t, Q_0^2) = \frac{-dt}{t} \Delta(t, Q_o^2) \sum_b \int dz \frac{\alpha_s}{2\pi} P_{ba}(z), \tag{19}$$

which implies

$$\Delta_a(Q^2, Q_0^2) = \exp\left[-\int_{Q_0^2}^{Q^2} \frac{dt}{t} \sum_b \int dz \frac{\alpha_s}{2\pi} P_{ba}(z) \right]. \tag{20}$$

The attendant non-branching probability appearing in the evolution equation is

$$\Delta(Q^2, t) = \frac{\Delta_a(Q^2, Q_o^2)}{\Delta_a(t, Q_o^2)}, \quad t = k_a^2 \quad \text{the virtuality of gluon } a. \tag{21}$$

The respective virtuality of parton a is then generated with

$$\Delta_a(Q^2, t) = R, \tag{22}$$

where R is a random number uniformly distributed in $[0, 1]$. With (note $\beta_0 = b_0|_{n_c=3}$ here, where n_c is the number of colors)

$$\alpha_s(Q) = \frac{2\pi}{b_0 \log\left(\frac{Q}{\Lambda}\right)}, \tag{23}$$

we get for example

$$\int_0^1 dz \frac{\alpha_s(Q^2)}{2\pi} P_{qG}(z) = \frac{4\pi}{2\pi b_0 \ln\left(\frac{Q^2}{\Lambda^2}\right)} \int_0^1 dz \frac{1}{2} \left[z^2 + (1-z)^2 \right]$$

$$= \frac{2}{3} \frac{1}{b_0 \ln\left(\frac{Q^2}{\Lambda^2}\right)}. \tag{24}$$

10

so that the subsequent integration over dt yields

$$
\begin{aligned}
I &= \int_{Q_0^2}^{Q^2} \frac{1}{3} \frac{dt}{t} \frac{2}{b_0 \ln\left(\frac{t}{\Lambda^2}\right)} \\
&= \frac{2}{3b_0} \ln \ln \frac{t}{\Lambda^2}\Big|_{Q_0^2}^{Q^2} \\
&= \frac{2}{3b_0} \left[\ln \left(\frac{\ln\left(\frac{Q^2}{\Lambda^2}\right)}{\ln\left(\frac{Q_0^2}{\Lambda^2}\right)} \right) \right].
\end{aligned}
\tag{25}
$$

Finally, introducing I into Eq. (20) yields

$$
\begin{aligned}
\Delta_a(Q^2, Q_0^2) &= \exp\left[-\frac{2}{3b_0} \ln \left(\frac{\ln\left(\frac{Q^2}{\Lambda^2}\right)}{\ln\left(\frac{Q_0^2}{\Lambda^2}\right)} \right) \right] \\
&= \left[\frac{\ln\left(\frac{Q^2}{\Lambda^2}\right)}{\ln\left(\frac{Q_0^2}{\Lambda^2}\right)} \right]^{-\frac{2}{3b_0}}.
\end{aligned}
\tag{26}
$$

If we now let $\Delta_a(Q^2, t) = R$, then

$$
\left[\frac{\ln\left(\frac{t}{\Lambda^2}\right)}{\ln\left(\frac{Q^2}{\Lambda^2}\right)} \right]^{\frac{2}{3b_0}} = R
\tag{27}
$$

which implies

$$
t = \Lambda^2 \left(\frac{Q^2}{\Lambda^2} \right)^{R^{\frac{3b_0}{2}}}.
\tag{28}
$$

Recall in HERWIG6.5 [8] we have

$$
\begin{aligned}
b_0 &= \left(\frac{11}{3} n_c - \frac{2}{3} n_f \right) \\
&= \frac{1}{3} \left(11 n_c - 10 \right), \quad n_f = 5 \\
&\equiv \frac{2}{3} \texttt{BETAF}
\end{aligned}
\tag{29}
$$

where in the last line we used the notation in HERWIG6.5. The momentum available after a $q\bar{q}$ split in HERWIG6.5 [8] is given by

$$
\texttt{QQBAR} = \texttt{QCDL3} \left(\frac{\texttt{QLST}}{\texttt{QCDL3}} \right)^{R^{\texttt{BETAF}}},
\tag{30}
$$

11

in complete agreement with Eq. (28) when we note the identifications $t = \texttt{QQBAR}^2$, $\Lambda \equiv$ $\texttt{QCDL3}$, $Q \equiv \texttt{QLST}$.

The leading log exercise leads to the same algebraic relationship that HERWIG6.5 has between $\texttt{QQBAR}$ and $\texttt{QLST}$ but we stress that in HERWIG6.5 these quantities are the angle-ordered counterparts of the virtualities we used in our example, so that the shower is angle-ordered.

Let us now repeat the above calculation for the IR-Improved kernels in Eq. (6). We have

$$P_{qG}^{\text{exp}}(z) = F_{\text{YFS}}(\gamma_G)e^{\delta_G/2}\frac{1}{2}\left[z^2(1-z)^{\gamma_G} + (1-z)^2 z^{\gamma_G}\right] \tag{31}$$

so that

$$\int_0^1 dz \frac{\alpha_s\left(Q^2\right)}{2\pi}P_{qG}(z)^{\text{exp}} = \frac{4F_{\text{YFS}}(\gamma_G)e^{\delta_G/2}}{b_0\ln\left(\frac{Q^2}{\Lambda^2}\right)(\gamma_G+1)(\gamma_G+2)(\gamma_G+3)}. \tag{32}$$

This leads to the following integral over dt:

$$\begin{aligned}
I &= \int_{Q_0^2}^{Q^2} \frac{dt}{t}\frac{4F_{\text{YFS}}(\gamma_G)e^{\delta_G/2}}{b_0\ln\left(\frac{t}{\Lambda^2}\right)(\gamma_G+1)(\gamma_G+2)(\gamma_G+3)} \\
&= \left.\frac{4F_{\text{YFS}}(\gamma_G)e^{\gamma_G/4}}{b_0(\gamma_G+1)(\gamma_G+2)(\gamma_G+3)}\text{Ei}\left(1,\frac{8.369604402}{b_0\ln\left(\frac{t}{\Lambda^2}\right)}\right)\right|_{Q_0^2}^{Q^2}.
\end{aligned} \tag{33}$$

We finally get the IR-improved formula

$$\Delta_a(Q^2,t) = \exp\left[-\left(F\left(Q^2\right) - F\left(t\right)\right)\right], \tag{34}$$

where

$$F(Q^2) = \frac{4F_{\text{YFS}}(\gamma_G)e^{\gamma_G/4}}{b_0(\gamma_G+1)(\gamma_G+2)(\gamma_G+3)}\text{Ei}\left(1,\frac{8.369604402}{b_0\ln\left(\frac{Q^2}{\Lambda^2}\right)}\right), \tag{35}$$

and Ei is the exponential integral function. In Fig. 2 we show the difference between the two results for $\Delta_a(Q^2,t)$. We see that they agree within a few percent except for the softer values of t, as expected. We look forward to determining definitively whether the experimental data prefer one over the other. This detailed study will appear elsewhere [43] but we begin the discussion below with a view on recent FNAL data. Again, we note that the comparison in Fig. 2 is carried out at the leading log virtuality level, but the sub-leading effects suppressed in this discussion will not change our general conclusions drawn therefrom.

For further illustration, we note that for the $q \to qG$ branching process in HER-WIG6.5 [8], we have therein the implementation of the usual DGLAP-CS kernel as follows:

12

```
            WMIN = MIN(ZMIN*(1. -ZMIN), ZMAX*(1.-ZMAX))
            ETEST = (1. + ZMAX**2) * HWUALF(5-SUDORD*2, QNOW*WMIN)
            ZRAT = ZMAX/ZMIN
      30    Z1 = ZMIN * ZRAT**HWRGEN(0)
            Z2 = 1. - Z1
            PGQW = (1. + Z2*Z2)
            ZTEST = PGQW * HWUALF(5-SUDORD*2, QNOW*Z1*Z2)
            IF (ZTEST .LT. ETEST*HWRGEN(1)) GOTO 30
            ...
```
$$(36)$$

where the branching of q to G at $z =$`Z1` occurs in the interval from `ZMIN` to `ZMAX` set by the inputs to the program and the current value of the virtuality `QNOW`, `HWUALF` is the respective function for α_s in the program and `HWRGEN(J)` are uniformly distributed random numbers on the interval from 0 to 1. It is seen that Eq. (36) is a standard MC realization of the unexponentiated DGLAP-CS kernel via

$$\alpha_s(Qz(1-z))P_{Gq}(z) = \alpha_s(Qz(1-z))\frac{1+(1-z)^2}{z} \qquad (37)$$

where the normalization is set by the usual conservation of probability. To realize this with the IR-improved kernel, we make the replacement of the code in Eq. (36) with the lines

```
            NUMFLAV = 5
            B0 = 11. - 2./3.*NUMFLAV
            L = 16./(3.*B0)
            DELTAQ = L/2 + HWUALF(5-SUDORD*2, QNOW*WMIN)*1.184056810
            ETEST = (1. + ZMAX**2) * HWUALF(5-SUDORD*2, QNOW*WMIN)
                  * EXP(0.5*DELTAQ) * FYFSQ(NUMFLAV-1) * ZMAX**L
            ZRAT = ZMAX/ZMIN
      30    Z1 = ZMIN * ZRAT**HWRGEN(0)
            Z2 = 1. - Z1
            DELTAQ = L/2 + HWUALF(5-SUDORD*2, QNOW*Z1*Z2)*1.184056810
            PGQW = (1. + Z2*Z2) * EXP(0.5*DELTAQ) * FYFSQ(NUMFLAV-1)
                  * Z1**L
            ZTEST = PGQW * HWUALF(5-SUDORD*2, QNOW*Z1*Z2)
            IF (ZTEST .LT. ETEST*HWRGEN(1)) GOTO 30
            ...
```
$$(38)$$

so that with the identifications $\gamma_q \equiv$ `L`, $\delta_q \equiv$ `DELTAQ`, $F_{\mathrm{YFS}}(\gamma_q) \equiv$ `FYFSQ(NUMFLAV - 1)`, we see that Eq. (38) realizes the IR-improved DGLAP-CS kernel $P_{Gq}^{\exp}(z)$ via $\alpha_s(Qz(1-z))P_{Gq}^{\exp}(z)$ with the normalization again set by probability conservation.

Continuing in this way, we have carried out the corresponding changes for all of the kernels in Eq. (6) in the HERWIG6.5 environment, with its angle-ordered showers, resulting in the new MC, HERWIRI1.0(31), in which the ISR parton showers have IR-improvement as given by the kernels in Eq. (18). In the original release of the program,

13

v. 1.0, we stated that the time-like parton showers had been completely IR-improved in a way that suggested the space-like parton showers had not yet been IR-improved at all. In the subsequent release, v. 1.02, the part of the space-like parton showers without IR-improvement associated with HERWIG6.5's space-like module HWSGQQ for the space-like branching process $G \to q\bar{q}$, a process which is not IR divergent and which is, in any case, a sub-dominant part of the shower, was IR-improved. In the release in version 1.031 the final missing IR-improvement in the space-like module HWSFBR[3] has been implemented. The IR-improvement of the module HWSGQQ in the release HERWIRI1.02 produces a small effect, as these considerations suggest: we see effects at a level comparable to the errors on the MC data in our plots when going from version 1.0 to 1.02. In going from version 1.0 to 1.031, we do some significant effects in the soft p_T regime so that we recommend the use of version 1.031 in comparison with data, as we illustrate presently.

We now illustrate some of the results we have obtained in comparing ISR showers in HERWIG6.5 and with those in HERWIRI1.0(31) at LHC and at FNAL energies, where some comparison with real data is also featured at the FNAL energy. Specifically, we compare the z-distributions, p_T-distributions, etc., that result from the IR-improved and usual DGLAP-CS showers in what follows [44].

First, for the generic 2→2 hard processes at LHC energies (14 TeV) we get the comparison shown Figs. 3, 4 for the respective ISR z-distribution and p_T^2 distribution at the parton level. Here, there are no cuts placed on the MC data and we define z as $z = E_{\mathrm{parton}}/E_{\mathrm{beam}}$ where E_{beam} is the cms beam energy and E_{parton} is the respective parton energy in the cms system. The two quantities z and p_T^2 for partons are of course not directly observable but their distributions show the softening of the IR divergence as we expect.

Turning next to the similar quantities for the π^+ production in the generic 2→2 hard processes at LHC, we see in Figs. 5, 6 that spectra in the former are similar and spectra in the latter are again softer in the IR-improved case. These spectra of course would be subject to some "tuning" in a real experiment and we await with anticipation the outcome of such an effort in comparison to LHC data.

We turn next to the luminosity process of single Z production at the LHC, where in Figs. 7,8,9 we show respectively the ISR parton energy fraction distribution, the Z p_T distribution, and the Z rapidity distribution with cuts on the acceptance as 40GeV $< M_Z$, $p_T^\ell > 5$GeV for $Z \to \mu^+\mu^-$ – all lepton rapidities are included. For the energy fraction distribution and the p_T distributions we again see softer spectra in the former

---

[3]We thank M. Seymour and B. Webber for discussion on this point.

and similar spectra in the latter in the IR-improved case. For the rapidity plot, we see the migration of some events to the higher values of Y, which is not inconsistent with a softer spectrum for the IR-improved case. One might wonder why we show the Z rapidity here as the soft gluons which we study only have an indirect affect on it via momentum conservation? But, this means that the rapidity predicted by the IR-improved showers should be close to that predicted by the un-improved showers and we show this cross-check is indeed fulfilled in our plots. To understand why one has the migration to higher values of rapidity in the IR-improved spectra, recall the IR-improved spectra move the radiated partons to softer values of z and this means the produced Z's have harder values of energy for given p_T as the p_T spectra are similar, and this in turn means these Z's have higher values of the rapidity variable. We look forward to the confrontation with experiment, where again we stress that in a real experiment, a certain amount of "tuning" will affect these results. We note for example that the difference between the spectra in Fig. 8, while it is interesting, is well within the range that could be tuned away by varying the amount of intrinsic transverse momentum of partons in the proton. The question will always be which set of distributions gives a better χ^2 per degree of freedom.

Finally, we turn the issue of the IR-cut-off in HERWIG6.5. In HERWIG6.5, there is are IR-cut-off parameters used to separate real and virtual effects and necessitated by the +-function representation of the usual DGLAP-CS kernels. In HERWIRI, these parameters in principle can be taken arbitrarily close to zero, as the IR-improved kernels are integrable [14, 15]. We note that in the current version of HERWIRI, the formula for $\alpha_s(Q)$ is unchanged from that in HERWIG6.5 so that there is still a Landau pole therein and this would prevent our taking the attendant IR cut-off parameters arbitrarily close to zero; however, we also note that this Landau pole is spurious and a more realistic behavior for $\alpha_s(Q)$ as $Q \rightarrow 0$ from either the lattice approach [45] or from other approaches such as those in Refs. [46, 47] could be introduced in the regime where the usual formula for $\alpha_s(Q)$ fails and this would allow us to approach zero with the IR cut-off parameters. With this understanding, we now illustrate the difference in IR-cut-off response by comparing it for HERWIG6.5 and HERWIRI: we change the default values of the parameters in HERWIG6.5 by factors of 0.7 and 1.44 as shown in the Fig. 10. We see that the harder cut-off reduces the phase space significantly only for the IR-improved kernels and that the softer cut-off has also a small effect on the usual kernels' spectra whereas as expected the IR-improved kernels' spectra move significantly toward softer values as a convergent integral would lead one to expect; for, one must note here that the spectra all stop at approximately the same value $z_0 \cong .00014 - .0016$ which is above some of the modulated IR-cut-off parameters and that the peaks in the spectra are not at the respective IR cut-off values which are defaulted [8] at $z = 0.000114$, 0.000121 for quarks and gluons, respectively, as the HERWIG environment has other built-in cut-offs that prevent such things as the α_s argument's becoming too small. What the curves in Fig. 10 show then are the relative "relative" probabilities for normalized spectra above z_0. Specifically, the areas under the six curves in the figure are all equal. The curves then show the difference in

the shapes of the parton energy spectra for the given values of the IR cut-off parameters when the interplay with the HERWIG environment's other built-in cut-offs to prevent unphysical phenomena from occurring in the simulation is taken into account. We can make an estimate of the attendant relative relative probabilities as follows. We compare the probability $P(z_0 < z < z_1)$ in a normalized spectrum for the spectra with the IR cut-offs in the usual case, where for soft gluon quanta we have $dP \sim dz'/z'$ in usual DGLAP-CS theory for the IR singular part, with the analogous probability in the IR-improved case, where for soft gluon quanta we have $dP \sim dz'/z'^{1-\gamma}$ with $\gamma = \gamma_A$, $A = q$, G. Considering the q case for definiteness, we have, for $z_0 \cong 0.00015$, an IR cut-off [8] $z_{cq} = 0.80\text{GeV}/7\text{TeV} \cong 0.000114$ as noted above, so that we need to compare the two relative probabilities

$$P(z_0 < z_q < z_1) = \begin{cases} \frac{\ln(1-z_0) - \ln(1-z_1)}{\ln(1-z_{cq}) - \ln(z_{cG})}, & \text{unimproved} \\ \frac{(1-z_0)^\gamma - (1-z_1)^\gamma}{(1-z_{cq})^\gamma - z_{cG}{}^\gamma}, & \text{IR-improved} \end{cases} \tag{39}$$

where we also introduced notation for the HERWIG environment gluon IR cut-off [8] $z_{cG} = 0.85\text{GeV}/7\text{TeV} \cong 0.000121$ with its default value. This shows that the two relative probabilities are in the ratio $r \cong (1 - z_{cG}{}^\gamma)/(-\gamma \ln(z_{cG}))$ so that the probability is enhanced in the IR-improved spectra. Putting in the numbers for we get $r \cong 0.16$ for the suppression of the unimproved spectrum relative to the IR-improved one. This is of course an overestimate of the effect because we only analyzed the IR singular terms in the soft regime but we see that the suppression effect is consistent with the plots in Fig. 10. If we want to be more complete, we also need to analyze the $\bar{q}$ and G singular cases and to take the suppression of the soft gluon spectrum in the IR-improved spectrum into account. Concerning the $\bar{q}$ case, it is the same as the q case – we get an enhancement of the soft region in the IR-improved spectrum relative to the unimproved one. For the gluon case, when the branching is $G \to G(z) + G(1 - z)$, for the part of the gluon branching kernel that is singular in z there is an enhancement in the relative probability that the gluon with fraction $1 - z$ will be in the soft region; the converse also holds. Finally, all of the soft gluon singularities are suppressed in the IR-improved cases relative to their unimproved cases, so that this will move particles away from the soft regime in the IR-improved cases relative to the unimproved cases. What is crucial to the Fig. 10 results is the interplay with the HERWIG6.5 environmental cut-offs such as that one on the argument of $\alpha_s = \alpha_s(Qz(1 - z))$ where Q is the HERWIG6.5 angle-ordered evolution variable. This cut-off on the variable $\mathcal{Q} = z(1 - z)Q$ means that the regime where either $z \to 0$ or $1 - z \to 0$ is suppressed in both sets of spectra. But, as the unimproved spectra have their largest enhancements in this regime relative to the IR-improved spectra, the HERWIG6.5 environment kills a large part of this enhancement and allows the other enhancements such as that in (39) to prevail, as we see in the figure. The behavior illustrated in Fig. 10 is expected to lead to a better description of the soft radiation data at LHC and this expectation should be checked with experiment in the not-too-distant future.

We finish this initial comparison discussion by turning to the data from FNAL on

the Z rapidity and p_T spectra as reported in Refs. [48, 49]. We show these results, for 1.96TeV cms energy, in Fig. 11. We see that HERWIRI1.0(31) and HERWIG6.5 both give a reasonable overall representation of the CDF rapidity data but that HERWIRI1.031 is somewhat closer to the data for small values of Y. The two χ^2/d.o.f are 1.77 and 1.54 for HERWIG6.5 and HERWIRI1.0(31) respectively. The data errors in Fig. 11(a) do not include luminosity and PDF errors [48], so that they can only be used conditionally at this point. We note as well that including the NLO contributions to the hard process via MC@NLO/HERWIG6.510 and MC@NLO/HERWIRI1.031 [33][4] improves the agreement for both HERWIG6.5 and for HERWIRI1.031, where the χ^2/d.o.f are changed to 1.40 and 1.42 respectively. That they are both consistent with one another and within 10% of the data in the low Y region is fully consistent with what we expect given our comments about the errors and the generic accuracy of an NLO correction in QCD. A more precise discussion at the NNLO level with DGLAP-CS IR-improvement and a more complete discussion of the errors will appear [43]. These rapidity comparisons are then important cross-checks on our work.

We also see that HERWIRI1.031 gives a better fit to the D0 p_T data compared to HER-WIG6.5 for low p_T, (for $p_T < 12.5$GeV, the χ^2/d.o.f. are ~ 2.5 and 3.3 respectively if we add the statistical and systematic errors), showing that the IR-improvement makes a better representation of QCD in the soft regime for a given fixed order in perturbation theory. We have also added the results of MC@NLO [33] for the two programs and we see that the $\mathcal{O}(\alpha_s)$ correction improves the χ^2/d.o.f for the HERWIRI1.031 in both the soft and hard regimes and it improves the HERWIG6.510 χ^2/d.o.f for p_T near 3.75 GeV where the distribution peaks. For $p_T < 7.5$GeV the χ^2/d.o.f for the MC@NLO/HERWIRI1.031 is 1.5 whereas that for MC@NLO/HERWIG6.510 is worse. These results are of course still subject to tuning as we indicated above.

5 Conclusions

We have introduced a new approach to QCD parton shower MC's based on the new IR-improved DGLAP-CS kernels in Refs. [14,15] and we have realized the new approach with the MC HERWIRI1.0(31) in the HERWIG6.5 environment. HERWIRI1.0(31) then sets the stage for the further implementation of the attendant [5] new approach to precision QED⊗QCD predictions for LHC physics by the introduction of the respective resummed residuals needed to improve systematically the precision tag to the 1% regime for such processes as single heavy gauge boson production, for example. Here, we already note that our new IR-improved MC, HERWIRI1.0(31), available at http://thep03.baylor.edu,

---

[4]We thank S. Frixione for helpful discussions with this implementation.

is expected to allow for a better χ^2 per degree of freedom in data analysis of high energy hadron-hadron scattering for soft radiative effects. By comparison with the D0 FNAL data of single Z production, we have given evidence that this is indeed the case. As one would expect, the integration of HERWIRI into MC@NLO is seamless, as one may replace HERWIG with HERWIRI directly. In both cases, MC@NLO/HERWIG and MC@NLO/HERWIRI, we see an improvement in the comparison with both the CDF rapidity data and the D0 p_T data on single Z production. We await further tests of the new approach, both at FNAL and at LHC.

Acknowledgments

References

[1] See for example S. Jadach *et al.*, in *Geneva 1995, Physics at LEP2, vol. 2*, pp. 229-298; preprint hep-ph/9602393, for a discussion of technical and physical precision.

[2] S. Haywood, P.R. Hobson, W. Hollik and Z. Kunszt, in *Proc. 1999 CERN Workshop on Standard Model Physics (and more) at the LHC, CERN-2000-004*, eds. G. Altarelli and M.L. Mangano,(CERN, Geneva, 2000) p. 122 ; H. Spiesberger, *Phys. Rev. D* **52** (1995) 4936 ; W.J. Stirling,"Electroweak Effects in Parton Distribution Functions", talk presented at ESF Exploratory Workshop, *Electroweak Radiative Corrections to Hadronic Observables at TeV Energies* , Durham, Sept., 2003 ; M. Roth and S. Weinzierl,*Phys. Lett. B* **590** (2004) 190; J. Blumlein and H. Kawamura, *Nucl. Phys. B* **708** (2005) 467; *Acta Phys. Pol. B* **33** (2002) 3719; W. J. Stirling et al., in *Proc. ICHEP04*, eds. H. Chen *et al.* (World Sci. Publ., Singapore, 2005) p. 527; A.D. Martin *et al.*, *Eur. Phys. J. C* **39** (2005) 155, and references therein.

[3] A. Kulesza *et al.*, in *PoS RADCOR2007*:001, 2007; A. Denner *et al.*, *ibid.*: 002, 2007; A. Denner *et al.*,*Nucl. Phys. B* **662** (2003) 299; G. Balossini et al., arXiv:0805.1129, and references therein.

[4] S. Dittmaier, in *Proc. LP09*, 2009, in press.

[5] C. Glosser, S. Jadach, B.F.L. Ward and S.A. Yost,*Mod. Phys. Lett. A***19**(2004) 2113; B.F.L. Ward, C. Glosser, S. Jadach and S.A. Yost, in *Proc. DPF 2004*, *Int. J. Mod. Phys. A* **20** (2005) 3735; in *Proc. ICHEP04, vol. 1*, eds. H. Chen *et al.*,(World. Sci. Publ. Co., Singapore, 2005) p. 588; B.F.L. Ward and S. Yost, preprint BU-HEPP-05-05, in *Proc. HERA-LHC Workshop*, CERN-2005-014; in *Moscow 2006, ICHEP, vol. 1*, p. 505; *Acta Phys. Polon. B* **38** (2007) 2395; arXiv:0802.0724, in *PoS RADCOR2007*: 038, 2007; B.F.L. Ward *et al.*, arXiv:0810.0723, in *Proc. ICHEP08*; arXiv:0808.3133, in *Proc. 2008 HERA-LHC Workshop*,DESY-PROC-2009-02, eds. H. Jung and A. De Roeck, (DESY, Hamburg, 2009)pp. 180-186, and references therein.

[6] S. Jadach and B.F.L. Ward, *Comput. Phys. Commun.* **56**(1990) 351; *Phys. Lett. B* **274** (1992) 470; S. Jadach et al., *Comput. Phys. Commun.* **102** (1997) 229; S. Jadach, W. Placzek and B.F.L Ward, *Phys. Lett. B* **390** (1997) 298; S. Jadach, M. Skrzypek and B.F.L. Ward,*Phys. Rev. D* **55** (1997) 1206; S. Jadach, W. Placzek and B.F.L. Ward, *Phys. Rev. D* **56** (1997) 6939; S. Jadach, B.F.L. Ward and Z. Was,*Phys. Rev. D* **63** (2001) 113009; *Comp. Phys. Commun.* **130** (2000) 260; S. Jadach et al., *ibid.***140** (2001) 432, 475.

[7] D. R. Yennie, S. C. Frautschi, and H. Suura, *Ann. Phys.* **13** (1961) 379; see also K. T. Mahanthappa, *Phys. Rev.* **126** (1962) 329, for a related analysis.

[8] G. Corcella *et al.*, hep-ph/0210213; *J. High Energy Phys.* **0101** (2001) 010; G. Marchesini et al., *Comput. Phys. Commun.***67** (1992) 465.

[9] S. Joseph *et al.*, *Phys. Lett. B***685** (2010) 283; arXiv:0910.0491.

[10] G. Sterman,*Nucl. Phys. B* **281** (1987) 310; S. Catani and L. Trentadue, *Nucl. Phys. B* **327** (1989) 323; *ibid.* **353** (1991) 183.

[11] See for example C.W. Bauer, A.V. Manohar and M.B. Wise, *Phys. Rev. Lett.* **91** (2003) 122001; C.W. Bauer *et al. Phys. Rev. D* **70** (2004) 034014.

[12] G. Altarelli and G. Parisi, *Nucl. Phys. B* **126** (1977) 298; Yu. L. Dokshitzer, *Sov. Phys. JETP* **46** (1977) 641; L. N. Lipatov, *Yad. Fiz.* **20** (1974) 181; V. Gribov and L. Lipatov, *Sov. J. Nucl. Phys.* **15** (1972) 675, 938; see also J.C. Collins and J. Qiu, *Phys. Rev. D***39** (1989) 1398 for an alternative discussion of DGLAP-CS theory.

[13] C.G. Callan, Jr., *Phys. Rev. D***2** (1970) 1541; K. Symanzik, *Commun. Math. Phys.* **18** (1970) 227, and in *Springer Tracts in Modern Physics*, **57**, ed. G. Hoehler (Springer, Berlin, 1971) p. 222; see also S. Weinberg, *Phys. Rev. D***8** (1973) 3497.

[14] B.F.L. Ward, *Adv. High Energy Phys.* **2008** (2008) 682312 ; DOI:10.1155/2008/682312.

[15] B.F.L. Ward, *Ann. Phys.* **323** (2008) 2147.

[16] N.E. Adam *et al.*, *J. High Energy Phys.* **0805** (2008) 062.

[17] N.E. Adam *et al.*, *J. High Energy Phys.* **0809** (2008) 133.

[18] C. Lee and G. Sterman, *Phys. Rev. D* **75** (2007) 014022.

[19] S.M. Abyat *et al.*, *Phys. Rev. D* **74** (2006) 074004.

[20] F. Berends et al., "Z Line Shape", in *Z Physics at LEP 1, v. 1*, CERN-89-08, eds. G. Altarelli, R. Kleiss, and C. Verzegnassi,(CERN, Geneva, 1989) p. 89, and references therein.

[21] R.K. Ellis *et al.*, *Phys. Lett. B***78** (1978) 281; *Nucl. Phys. B* **152** (1979) 285; D. Amati, R. Petronzio and G. Veneziano, *ibid.***146** (1978) 29; S.B. Libby and G. Sterman, *Phys. Rev. D* **18** (1978) 3252; A.H. Mueller, *ibid.* **18** (1978) 3705.

[22] B.I. Ermolaev, M. Greco and S.I. Troyan, *PoS* **DIFF2006** (2006) 036, and references therein.

[23] G. Altarelli, R.D. Ball and S. Forte, *PoS* **RADCOR2007** (2008) 028.

[24] B.F.L Ward *et al.*, arXiv:0810.0723, 0808.3133.

[25] E.G. Floratos, D.A. Ross, C. T. Sachrajda, *Nucl. Phys. B* **129**(1977) 66;*ibid.***139**(1978) 545; *ibid.***152** (1979) 493,1979; A. Gonzalez-Arroyo, C. Lopez and F.J. Yndurain, *Nucl. Phys. B***153** (1979) 161; A. Gonzalez-Arroyo and C. Lopez, *Nucl. Phys. B* **166** (1980) 429; G. Curci, W. Furmanski and R. Petronzio, *Nucl. Phys. B* **175** (1980) 27; W. Furmanski and R. Petronzio, *Phys. Lett. B* **97** (1980) 437; E.G. Floratos, C. Kounnas and R. Lacaze, *Nucl. Phys. B* **192** (1981) 417; R. Hamberg and W. Van Neerven, *Nucl. Phys. B* **379** (1992) 143; S. Moch, J.A.M. Vermaseren and A. Vogt, *Nucl. Phys. B* **688** (2004) 101; *ibid.* **691** (2004) 129.

[26] See for example A. Cooper-Sarkar *et al.* in *Proc. 2006 - 2008 HERA-LHC Workshop*, DESY-PROC-2009-02, eds. H. Jung and A. De Roeck,(DESY, Hamburg, 2009) p. 74; T. Carli *et al.*, in *Proc. HERA-LHC Wkshp*, 2005.

[27] C. Di'Lieto, S. Gendron, I.G. Halliday, and C.T. Sachradja, *Nucl. Phys. B* **183** (1981) 223; R. Doria, J. Frenkel and J.C. Taylor, *ibid.***168** (1980) 93, and references therein.

[28] S. Catani, M. Ciafaloni and G. Marchesini, *Nucl. Phys.* **B264**(1986) 588; S. Catani, *Z. Phys.* **C37** (1988) 357.

[29] B.F.L. Ward, *Phys. Rev. D***78** (2008) 056001.

[30] U. Baur, S. Keller and W.K. Sakumoto, *Phys. Rev. D* **57** (1998) 199; U. Baur, S. Keller and D. Wackeroth, *ibid.***59** (1998) 013002; U. Baur *et al.*, *ibid.***65** (2002) 033007; S. Dittmaier and M. Kramer, *Phys. Rev. D* **65** (2002) 073007; and Z. A. Zykunov,*Eur. Phys. J. C***3** (2001) 9.

[31] R. Hamberg, W. L. van Neerven and T Matsuura, *Nucl. Phys. B***359** (1991) 343; W.L. van Neerven and E.B. Zijlstra, *Nucl. Phys. B* **382** (1992) 11; *ibid.* **680** (2004) 513; and C. Anastasiou et al., *Phys. Rev. D* **69** (2004) 094008.

[32] T. Sjostrand et al., hep-ph/0308153.

[33] S. Frixione and B.Webber, *J. High Energy Phys.* **0206** (2002) 029; S. Frixione, P. Nason and B. Webber, *ibid.* **0308** (2003) 007.

[34] S. Jadach and M. Skrzypek, *Comput. Phys. Commun.* **175** (2006) 511; P. Stevens et al., *Acta Phys. Polon. B* **38** (2007) 2379, and references therein.

[35] We thank M. Seymour and B. Webber for discussion on this point.

[36] B. Webber and M. Seymour, private communication.

[37] M. Hejna et al., to appear.

[38] M. Bahr *et al.*, arXiv:0812.0529 and references therein.

[39] F. Olness, private communication; P.M. Nadolsky *et al.*, arXiv:0802.0007.

[40] R. Thorne, private communication; A.D. Martin *et al.*, arXiv:0901.0002 and references therein.

[41] B.R. Webber, *Ann. Rev. Nucl. Part. Sci.* **36** (1986) 253-286.

[42] T. Sjostrand, *Phys. Lett. B***157**(1985) 321.

[43] S. Joseph *et al.*, to appear.

[44] Note that similar results for PYTHIA and MC@NLO are in progress.

[45] P. Boucaud *et al.*, *Nucl. Phys. B Proc. Suppl.* **106** (2002) 266; J. Skullerud, A. Kizilersu and A.G. Williams, *ibid.* **106** (2002) 841, and references therein.

[46] M. Baldicchi *et al.*, *Phys. Rev. Lett.* **99** (2007) 242001; D.V. Shirkov and I.L. Solovtsov, *ibid.* **79** (1997) 1209; R. Alkofer and L. von Smekal, *Phys. Rept.* **353** (2001) 281, and references therein.

[47] P.M. Brooks and C.J. Maxwell, *Phys. Rev. D* **74** (2006) 065012, and references therein.

[48] C. Galea, in *Proc. DIS 2008*, London, 2008, http://dx.doi.org/10.3360/dis.2008.55.

[49] V.M. Abasov *et al.*, *Phys. Rev. Lett.* **100**, 102002 (2008).
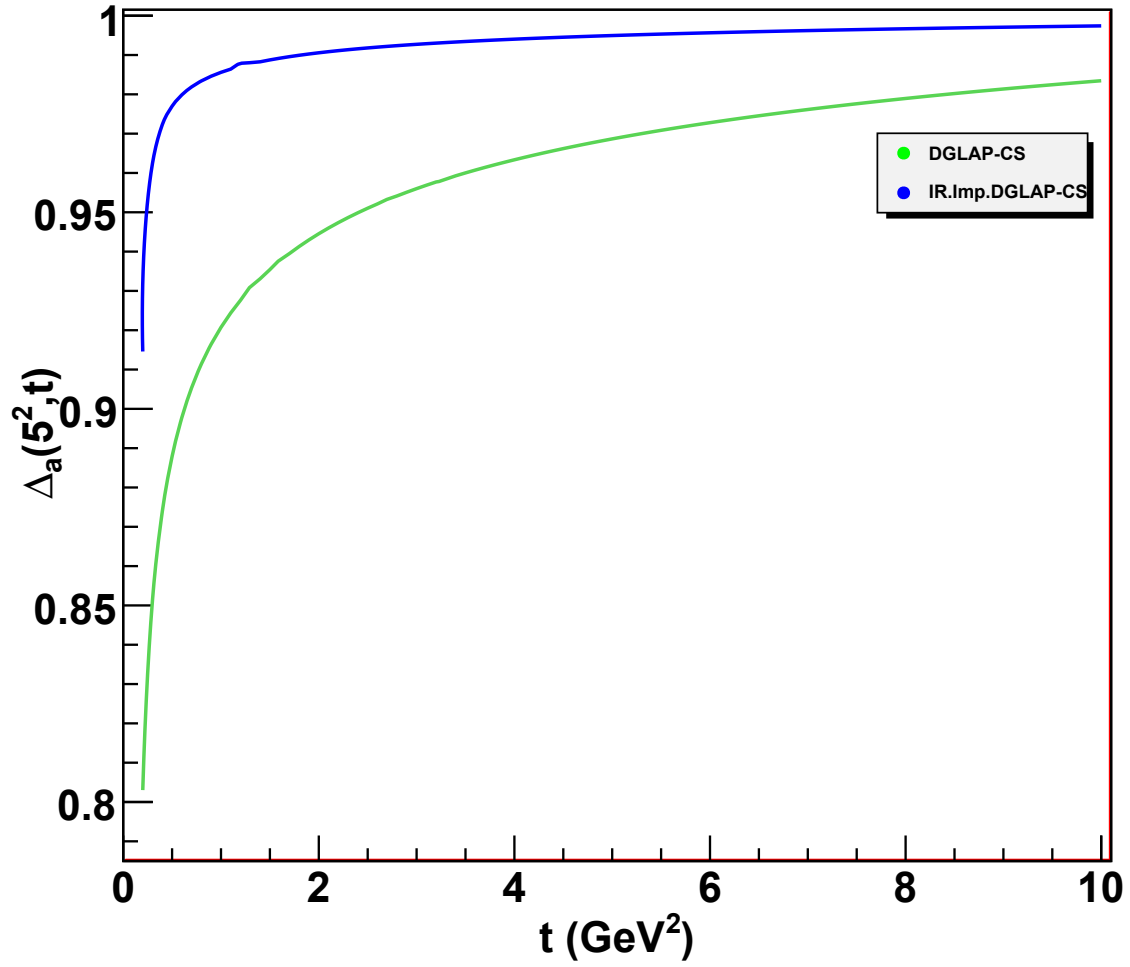
Figure 2: Graph of $\Delta_a(Q^2, t)$ for the DGLAP-CS and IR-Improved DGLAP-CS kernels Eqs. (26, 34). Q^2 is a typical virtuality close to the squared scale of the hard sub-process – here we use $Q^2 = 25\mathrm{GeV}^2$ for illustration.
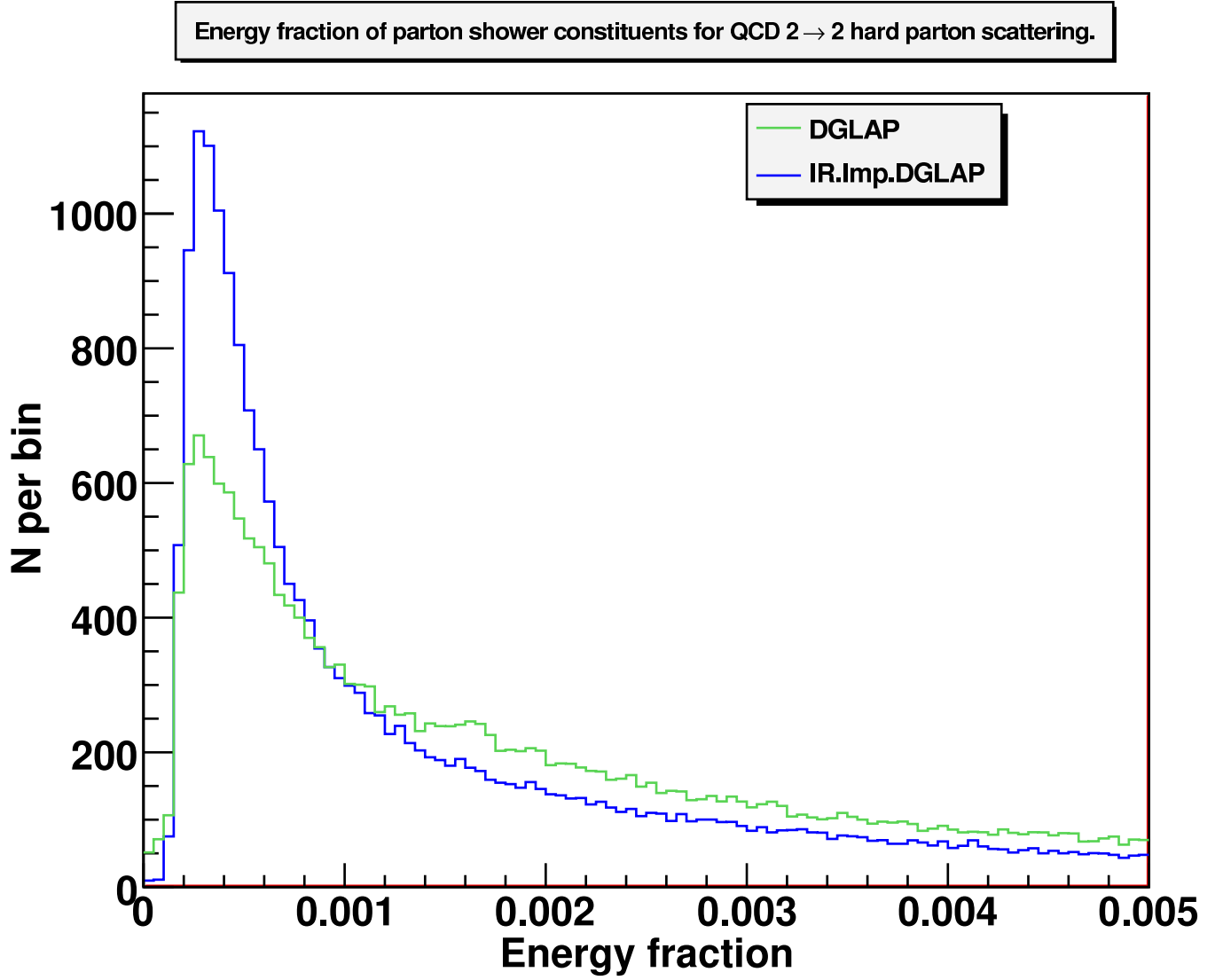
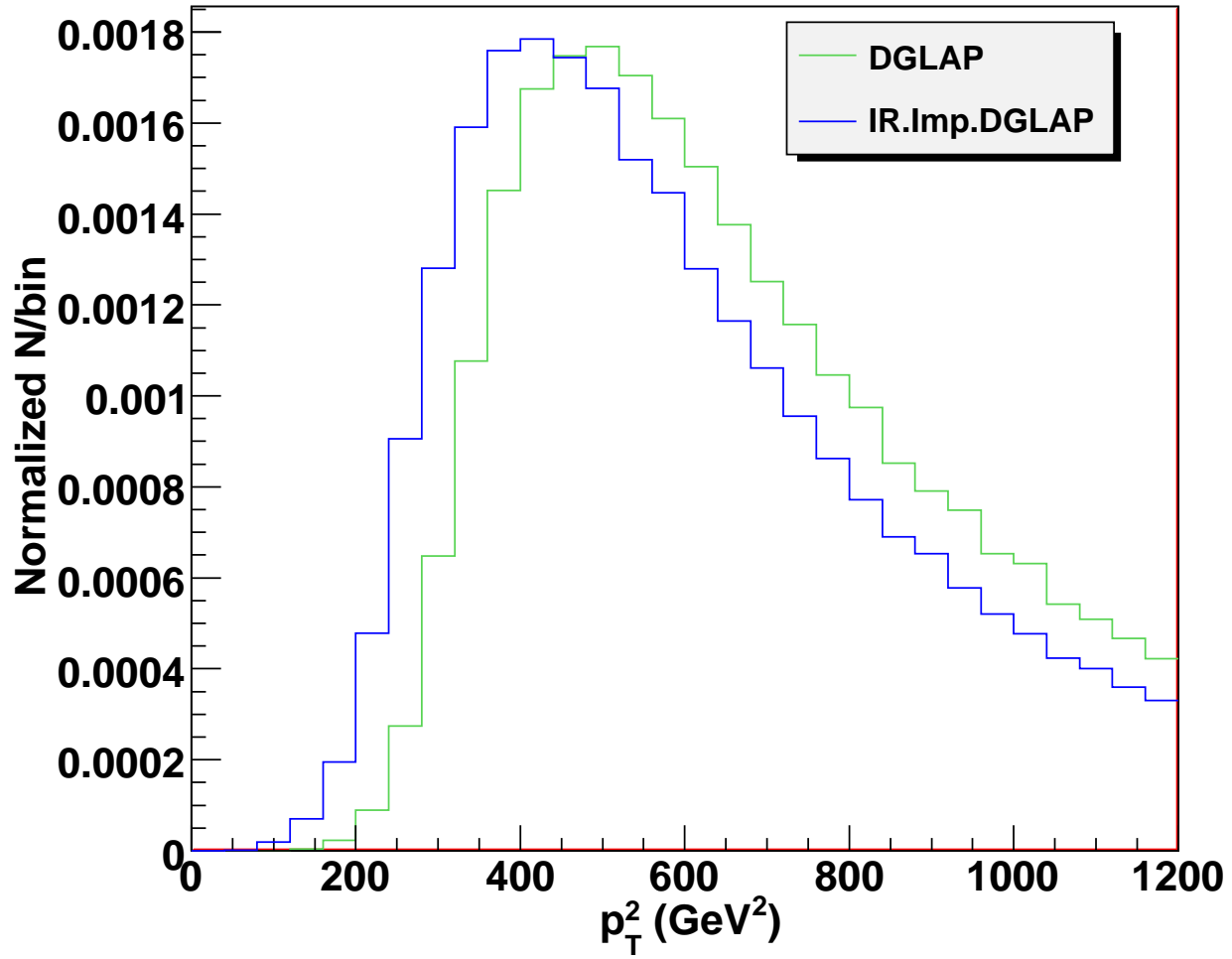Figure 3: The z-distribution(ISR parton energy fraction) shower comparison in HER-WIG6.5.

Figure 4: The p_T^2-distribution (ISR parton) shower comparison in HERWIG6.5.
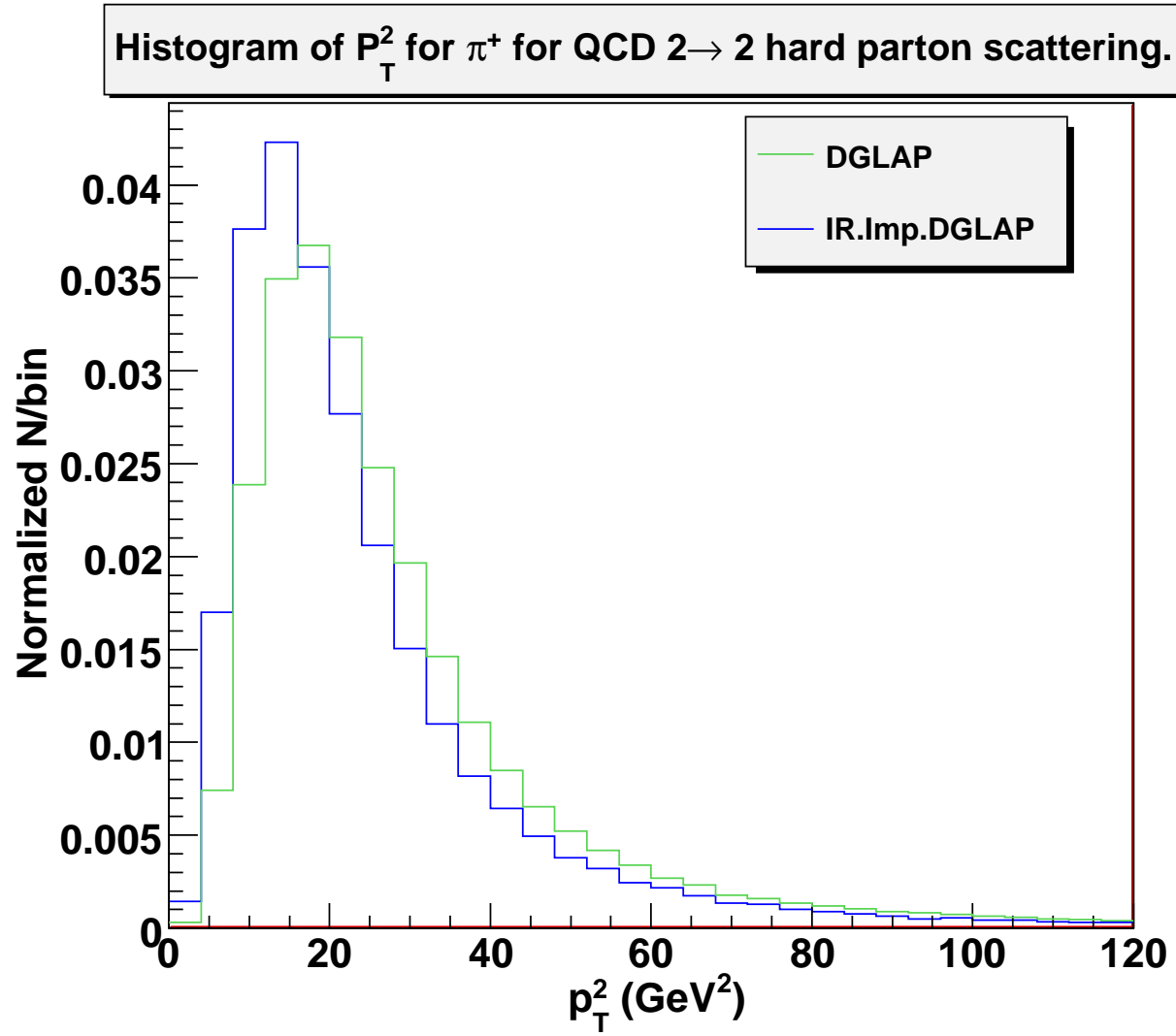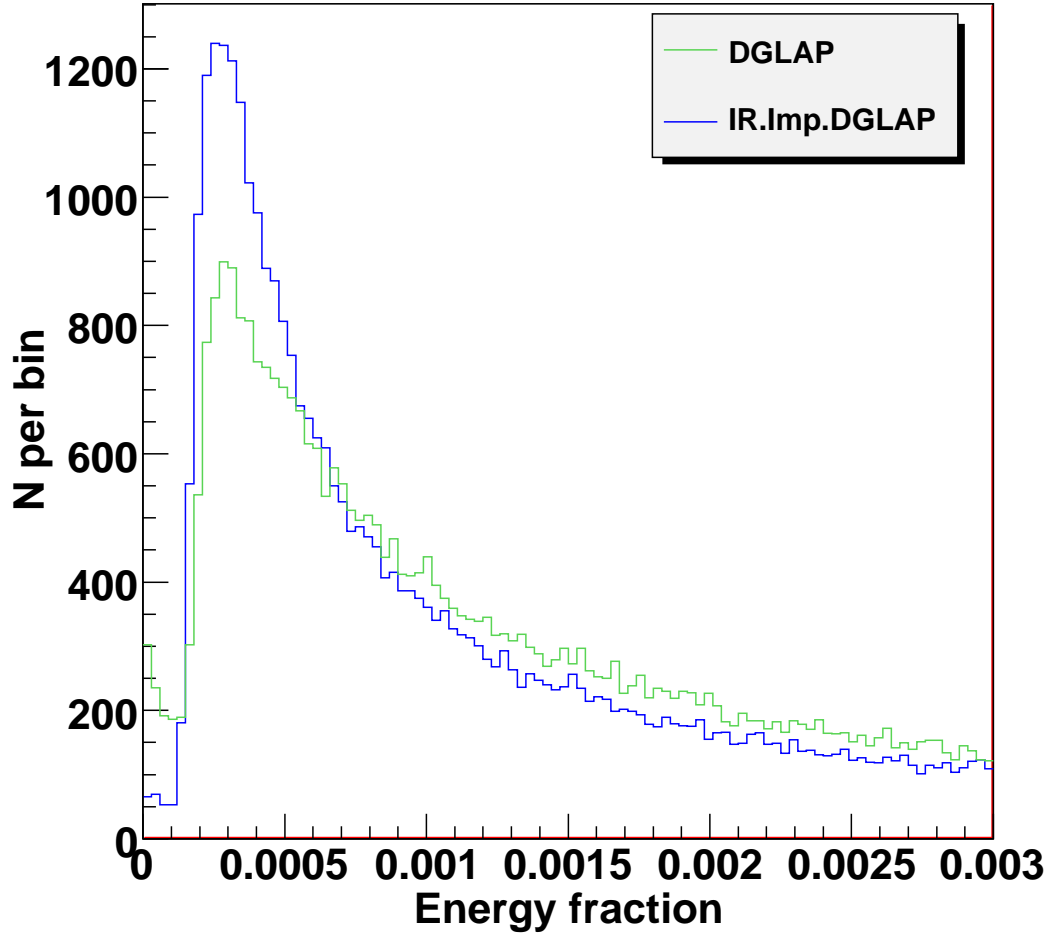
Figure 5: The π^+ energy fraction distribution shower comparison in HERWIG6.5.

Figure 6: The π^+ p_T^2-distribution shower comparison in HERWIG6.5.

Figure 7: The *z*-distribution(ISR parton energy fraction) shower comparison in HER-WIG6.5.

Figure 8: The Z p_T-distribution(ISR parton shower effect) comparison in HERWIG6.5.

The unit normalized differential cross section for Z production as a function of vector boson rapidity.
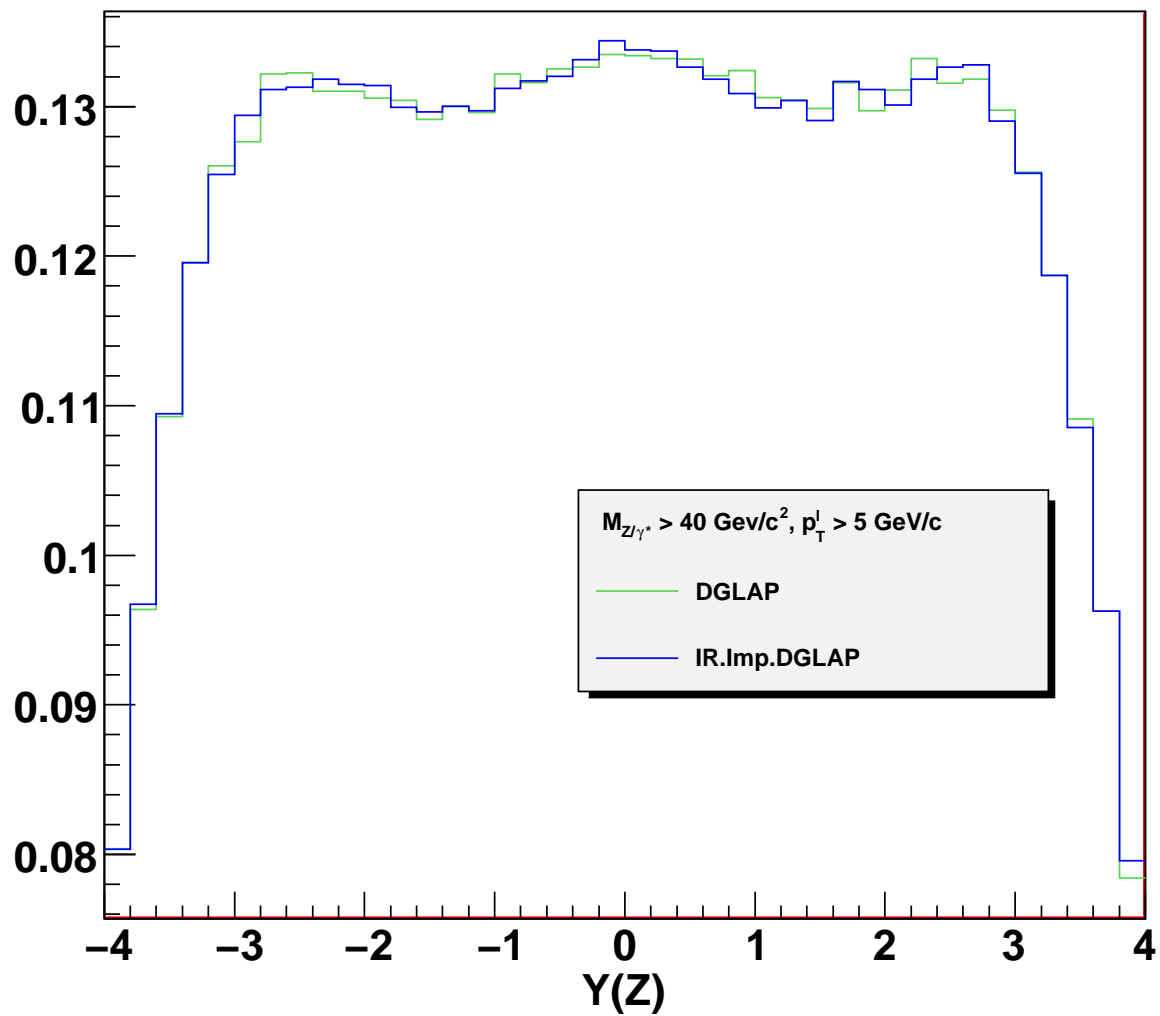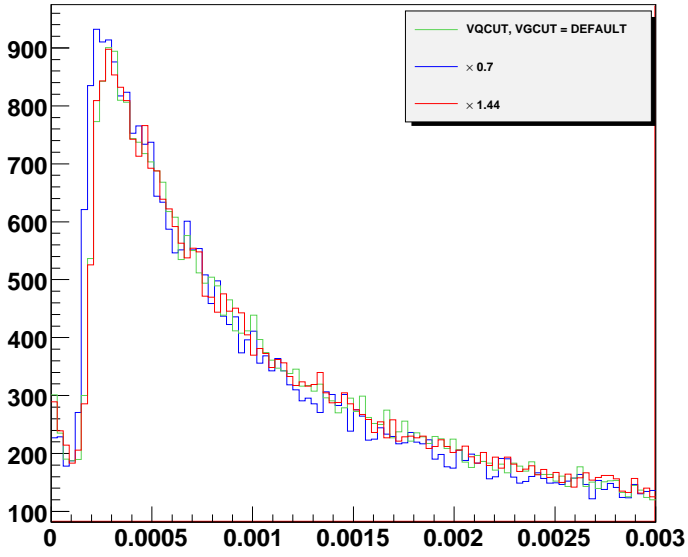
$M_{Z/\gamma^*} > 40$ Gev/c^2, $p_T^l > 5$ GeV/c

DGLAP

IR.Imp.DGLAP

Figure 9: The Z rapidity-distribution(ISR parton shower) comparison in HERWIG6.5.
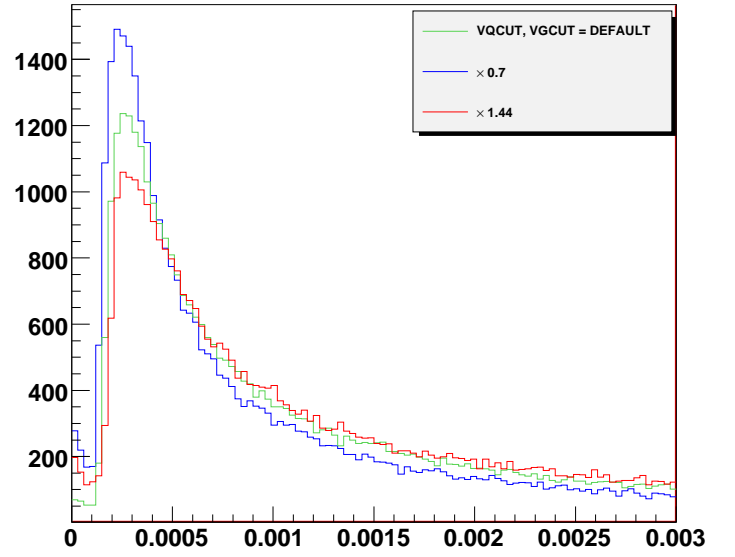
(a) **(b)**

Figure 10: IR-cut-off sensitivity in z-distributions of the ISR parton energy fraction: (a), DGLAP-CS (b), IR-I DGLAP-CS – for the single Z hard sub-process in HERWIG-6.5 environment.
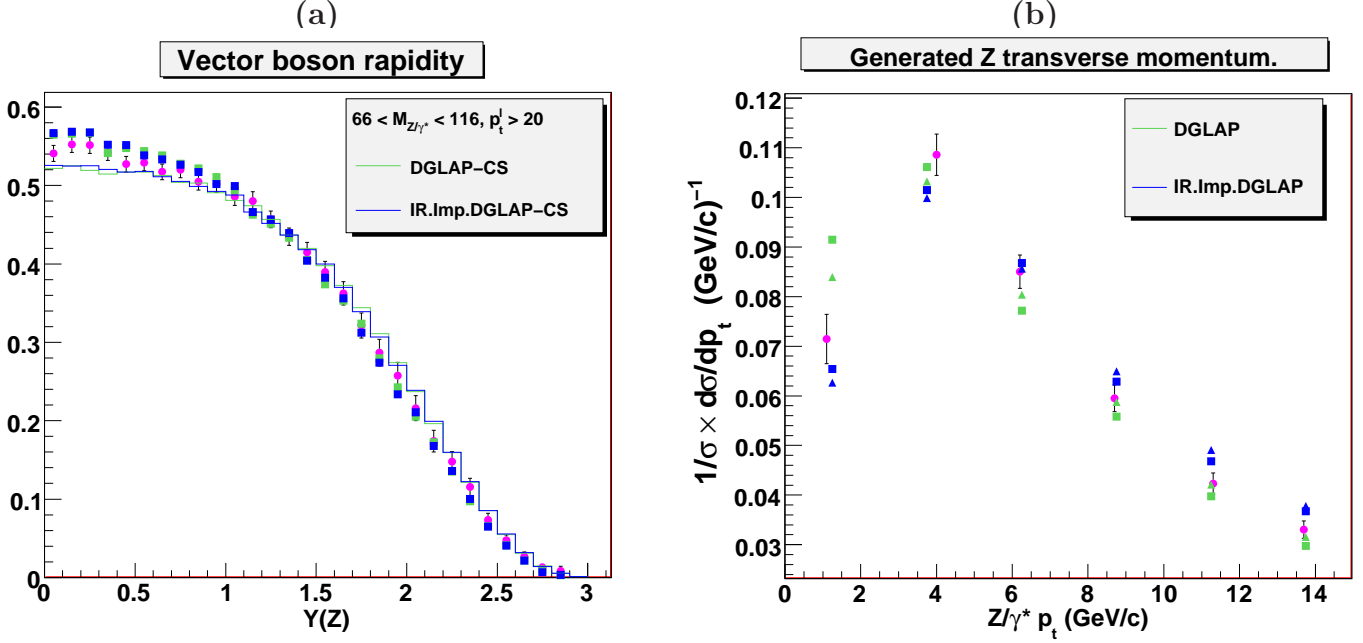
(a)

Vector boson rapidity

$66 < M_{Z/\gamma^*} < 116,\ p_t^l > 20$

DGLAP–CS

IR.Imp.DGLAP–CS

Y(Z)

(b)

Generated Z transverse momentum.

DGLAP

IR.Imp.DGLAP

$1/\sigma \times d\sigma/dp_t$ (GeV/c)$^{-1}$

$Z/\gamma^*\ p_t$ (GeV/c)

Figure 11: Comparison with FNAL data: (a), CDF rapidity data on (Z/γ^*) production to e^+e^- pairs, the circular dots are the data, the green(blue) lines are HERWIG6.510(HERWIRI1.031); (b), D0 p_T spectrum data on (Z/γ^*) production to e^+e^- pairs, the circular dots are the data, the blue triangles are HERWIRI1.031, the green triangles are HERWIG6.510. In both (a) and (b) the blue squares are MC@NLO/HERWIRI1.031, and the green squares are MC@NLO/HERWIG6.510, where we use the notation (see the text) MC@NLO/X to denote the realization by MC@NLO of the exact $\mathcal{O}(\alpha_s)$ correction for event generator X. Note that these are untuned theoretical results.